Journal of Molecular Liquids 390 (2023) 122947

Contents lists available at ScienceDirect

Journal of Molecular Liquids

journal homepage: www.elsevier.com/locate/molliq

Immobilization of pectinase on chitosan-alginate-clay composite beads: Experimental, DFT and molecular docking studies

Aysun Aksu [a], Serap Çetinkaya [a], Ali Fazıl Yenidünya [a], Şenay Akkuş Çetinus [b], Hayreddin Gezegen [c], Burak Tüzün [d,*]

[a] Department of Molecular Biology and Genetics, Science Faculty, Sivas Cumhuriyet University, Sivas, Turkey
[b] Department of Biochemistry, Faculty of Science, Sivas Cumhuriyet University, Sivas, Turkey
[c] Sivas Cumhuriyet University, Faculty of Health Sciences, Department of Nutrition and Dietetics, 58140 Sivas, Turkey
[d] Plant and Animal Production Department, Technical Sciences Vocational School of Sivas, Sivas Cumhuriyet University, Sivas, Turkey

ARTICLE INFO

Keywords:
Alginate
Chitosan
DFT
Immobilization
Molecular docking
Pectinase

ABSTRACT

Pectinase was immobilized on chitosan-alginate-clay (CAC) beads using epichlorohydrin (ECH) as the crosslinker. Prepared beads and immobilization product were analyzed by Fourier Transform Infrared Spectrophotometry (FTIR) and Scanning Electron Microscopy (SEM). Experimental data covered some hydrolytic properties of the immobilized enzyme, such as pH, temperature, reusability, concentration, and storage time. The immobilization procedure increased the optimal temperature to 60 °C and maximum activity was obtained at pH (6.0). After 5 cycles of reuse, approximately 45% of the initial activity of the immobilized enzyme remained. Free pectinase, CAC, and immobilization product were also investigated by Gaussian calculations, the HF/6-31g basis set. Furthermore, *Aspergillus niger* proteins (PDB ID: 3K4P and 7BLY) and Staphylococcus aureus (PDB ID: 1JIJ) were examined for molecular docking calculations, and ADME/T calculations were made to examine the effects and reactions of these molecules in human metabolism.

1. Introduction

Enzymes are biocatalytic proteins [1,2]. Commercial biocatalysts are often obtained from renewable microbial biomass [3–5]. Compared with conventional catalysts, enzymes also display stereo-, regio-, chemo- and enantio-selectivity on the substrate molecules [6]. Currently more than 4,000 enzymes have been exploited in industries involving biotechnological means [7–9].

Immobilization involves technologies used to improve the stability and reusability of enzymes [10–12], and to eliminate byproduct contamination [13,14]. The procedure often allows the enzyme to be bound on a solid support. The biochemistry of immobilized enzymes is inevitably reformatted by the nature of the support composite by means of its functional groups, and surface topology [15,16]. Therefore, the choice of the support/matrix is crucial [9,17–20].

Cost-effective alginate, cellulose, chitin, and chitosan biopolymers are inherently nontoxic, biodegradable, and biocompatible [21,22]. Their amine, carbonyl, and hydroxyl moieties underpin the high affinity binding to proteinaceous molecules [23,24]. Based on intermolecular reactions, enzymes are covalently crosslinked to support materials using a crosslinker [25].

Theoretical calculations are often used to predict the activities of molecules, and to develop and amplify their active sites [26]. In the calculations, various levels and base sets of ligand and metal complexes were calculated [27]. The interaction of molecules with *Aspergillus niger* proteins was examined and the best adherent molecules were determined. First, the activities of each studied molecule on the HF/6-31g basis set were investigated by Gaussian calculations. Comments were then made on their activities using various parameters. Furthermore, the molecular interactions with *Aspergillus niger* protein (PDB ID: 3K4P and 7BLY) [28,29] and Staphylococcus aureus (PDB ID: 1JIJ) [30], were examined by molecular docking calculations. Finally, ADME/T calculations were performed to examine the influences and reactions of these molecules in human body.

In this study, the pectinase (E.C.3.2.1.15) enzyme, which depolymerizes pectic polymers by hydrolysing the α-1,4-glycosidic bonds was used [31]. The work involved covalent bonding of pectinase on epichlorohydrin (ECH) activated chitosan-alginate-clay (CAC) matrix.

* Corresponding authors.
E-mail address: btuzun@cumhuriyet.edu.tr (B. Tüzün).

https://doi.org/10.1016/j.molliq.2023.122947
Received 14 May 2023; Received in revised form 17 August 2023; Accepted 27 August 2023
Available online 30 August 2023

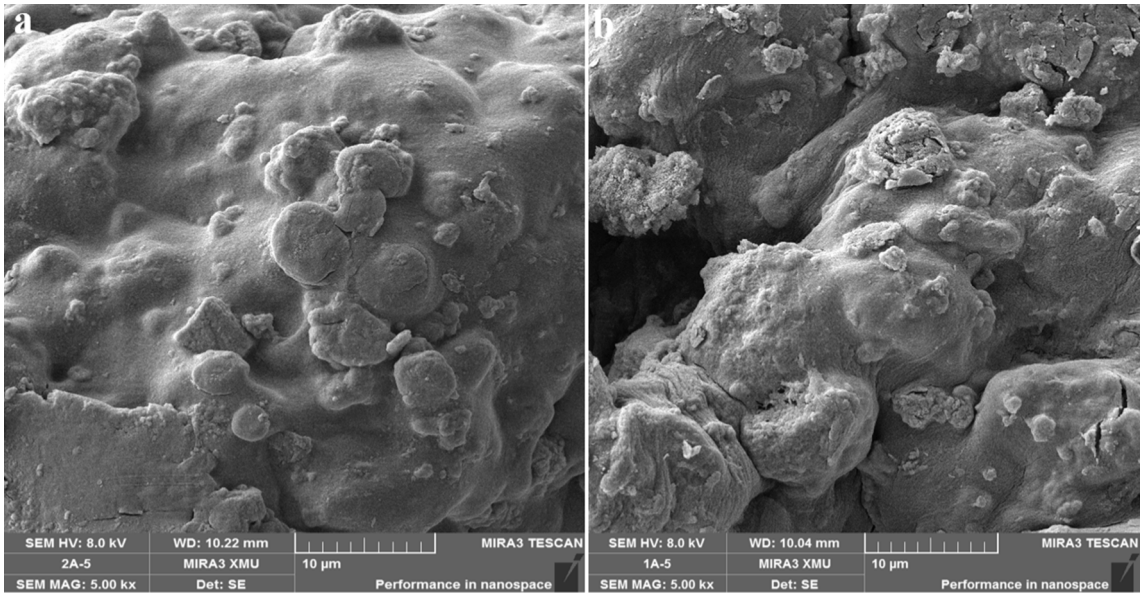

Fig. 1. SEM images of CAC composite before (a) and after immobilization (b).

The main advantage of using ECH as the crosslinking agent was that it could significantly improve the strength of wet chitosan films [32,33].

Immobilization product was analysed by FTIR spectroscopy, while changes in surface topology were inspected by SEM. Experimental work characterised some hydrolytic and biochemical properties of the immobilized enzyme: pH, temperature, reusability, concentration, and storage time. The immobilization procedure increased the optimal temperature to 60 °C and maximum activity was obtained at pH (6.0).

2. Material and methods

2.1. Materials

Chitosan, epichlorohydrin (ECH), sodium tripolyphosphate (NaTPP), 3,5-dinitrosalicylic acid, *Aspergillus niger* pectinase (1.18 U/mg), polygalactronic acid (≥90% enzymatic) were from Sigma Aldrich (St. Louis, MO, USA). Sodium alginate was from Isolab Chemicals (Eschau, GERMANY).

2.2. Synthesis of CAC matrix

Double-crosslinked CAC was prepared as follows: in 200 mL acetic acid (5%, v/v), equal amounts, 4 g, of chitosan, sodium alginate, clay were mixed at 25 °C. The resulting suspension was stirred for 2 h. Afterwards, 160 mL (0.01 M) epichlorohydrin (pH 10.0) was added to the suspension and the suspension was stirred vigorously for 1 h. Beads were formed by dropwise adding the suspension into 0.05 M sodium tripolyphosphate (NaTPP, 500 mL). The mixture was stirred for 3 h at 100 rpm. The beads were filtered, washed for 1 h in distilled water. Washing procedure was repeated thrice to get rid of excess NaTPP. The recovered beads were dried at 37 °C and stored at room temperature [34,35].

2.3. Immobilization of pectinase on CAC beads

Two hundred milligrams of beads were suspended for 4 h at 4 °C in 0.1 M sodium acetate (10 mL, pH 5.0) solution, containing 10 mg of pectinase. The beads were then washed with 0.1 M sodium acetate (pH 5.0), and stored in 0.1 mM sodium acetate (2 mL, pH 5) at + 4 °C. Before use, the beads were dried at 37 °C [36].

2.4. Structural analysis

2.4.1. FTIR and SEM

FTIR (4000–400 cm^{-1}, Perkin Elmer 400) and SEM (TESCAN MIRA3 XMU) analyses were performed at CÜTAM Central Laboratory (Sivas Cumhuriyet University).

2.5. Pectinase experiments

2.5.1. Protein content and pectinase activity assays

Protein concentration was determined by using Bradford method [37]. Immobilization efficiency was taken as the difference in protein content before and after immobilization.

2.5.2. Determination of enzyme activity by DNS method

The pectinolytic reaction was performed for 30 min at 37 °C in a shaker incubator. After cooling at room temperature, the solution was read at 575 nm (Shimadzu UV-1800 Japan). The amount of liberated reducing sugar was calculated as D-galacturonic acid equivalents [38].

The enzyme activity of free and immobilized pectinase was determined by adding 150 μL of enzyme solution into 600 μL of 1% w/v polygalacturonic acid in 0.1 M sodium acetate buffer (pH 5.0). The same amount of enzyme protein was used for the immobilized samples. The reaction was performed for 30 min at 37 °C in a shaking incubator, and then terminated with 3,5-dinitrosalicylic acid. The reaction sample was boiled for 10 min and read at 575 nm [39]. The following formulas were used for the activity calculations (Eqs. 1–3).

$$U/mL = \frac{w(\text{The amount of G.A. released (OD 575 nm/standard graph)})\text{*React. solut. vol.*D.F.}}{\text{Enzyme volume (ml)*Reaction time (min)}} \quad [1]$$

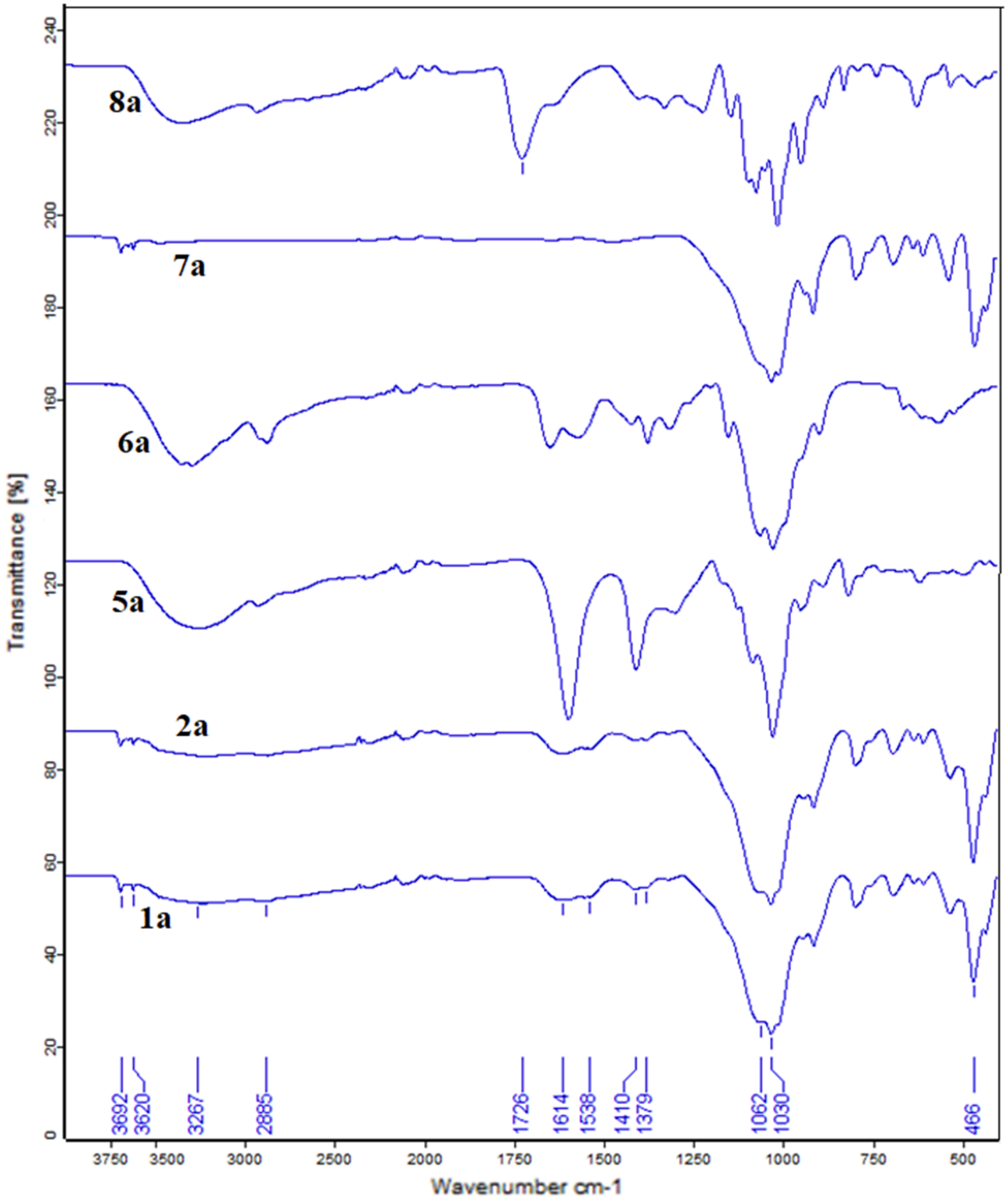

Fig. 2. FTIR spectra of 1a) pectinase immobilized on CAC; 2a) CAC; 5a) alginate; 6a) chitosan; 7a) clay; and 8a) polygalacturonic acid.

Table 1
Pectinase immobilization to CAC composite.

Volume Activity (μmol /ml)	Protein		Specific Activity (μmol mg protein^{-1} min^{-1})
Free Enzyme	2,274	10 mg/ml	0.2274
Immobilized Enzyme	0.00161	0.033 (mg protein/mg carrier)	0.0488

$$\text{Specific Activity} = \text{U}/mgprotein \quad [2]$$

$$\text{Relative Activity} = \text{Specific Activity}/\text{Optimum Specific Activity x 100} \quad [3]$$

2.6. Effects of pH and temperature

Free and immobilized enzymes were tried in different buffers (0.1 M sodium acetate/acetic acid, pH 3.0–6.0 and 0.1 M Na_2HP0_4/NaH_2PO_4, pH 7.0–8.0) for 30 min at 37 °C and at different temperatures ranging between 25 and 60 °C [40].

2.7. Kinetic calculations

Using the measurements of reaction rates, under optimum conditions, corresponding to different polygalacturonic acid concentrations (0.1–3%), V_{max} and K_m of the free and bound enzyme were plotted as Lineweaver-Burk curves [40].

Table 2
Kinetic parameters.

	K_m (% w/v)	V_{max} (μmol mg protein^{-1} min^{-1})
Free	0.273	3.10
İmmobilized	0.310	5.42 x10^{-2}

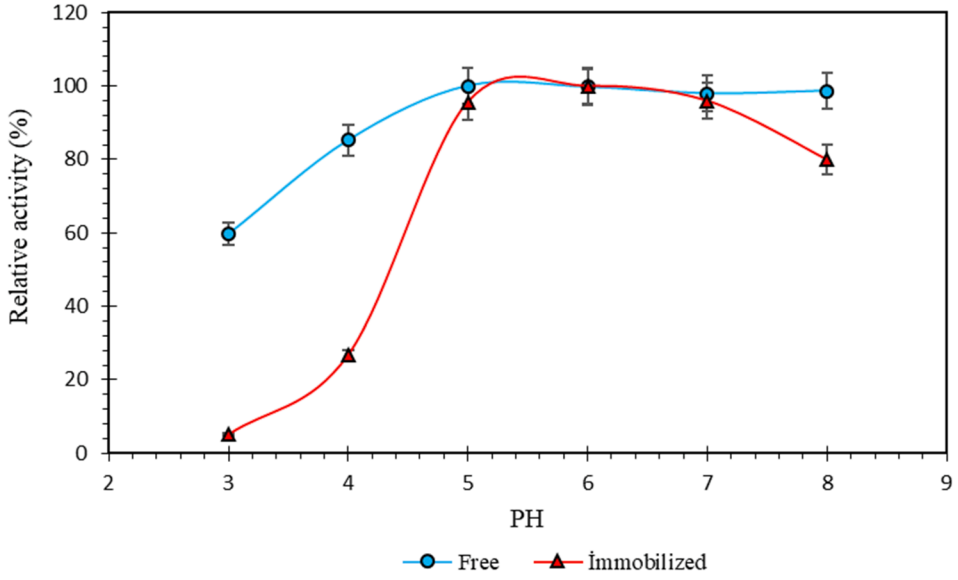

Fig. 3. Optimum pH of free- and immobilized pectinase.

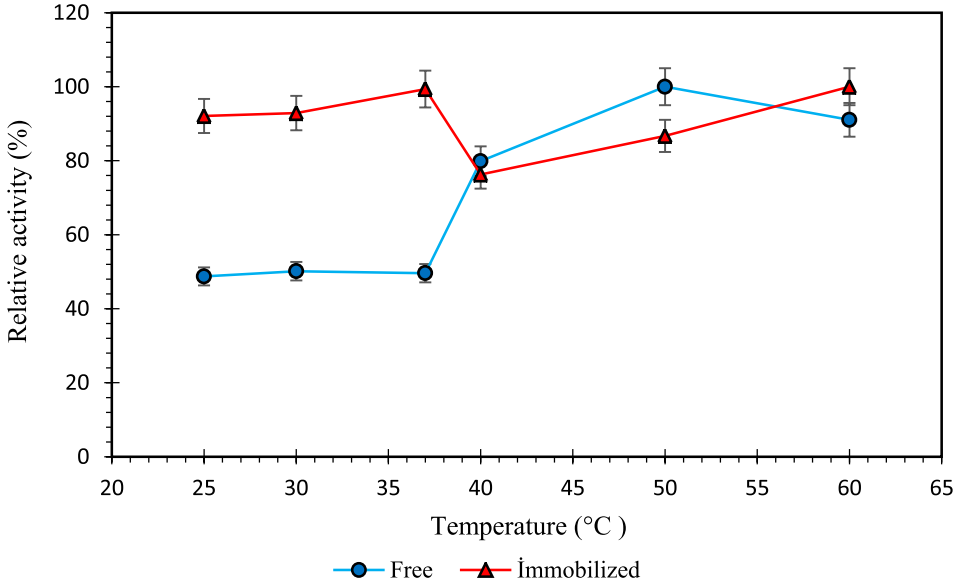

Fig. 4. Influence of temperature on the hydrolytic activity.

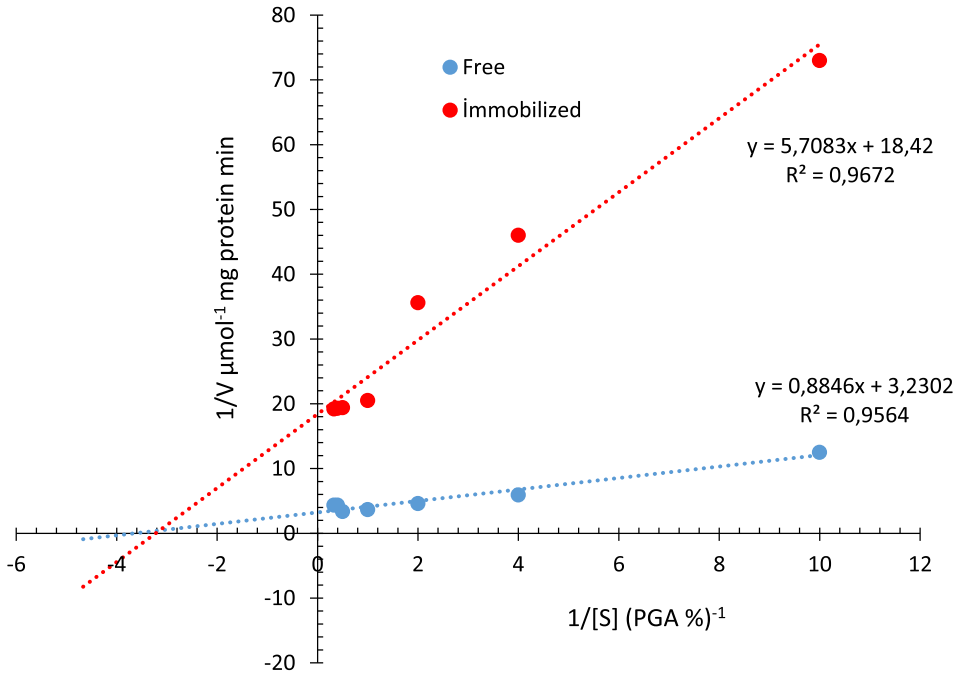

Fig. 5. Lineweaver Burk curve of free- and immobilized pectinase.

2.8. Reusability

One percent polygalacturonic acid (prepared in 0.1 mM acetate buffer, pH 5.0) was hydrolysed by interaction with immobilized pectinase for 30 min at 37 °C at 120 rpm. The immobilized pectinase was then washed with acetate (pH 5.0) and the hydrolytic reaction was repeated six times.

2.9. Immobilization time and enzyme concentration

Optimum immobilization time was determined by calculating the relative activity. In addition, different amounts of enzymes (5, 10, 20, 4, 8, mg/ml) were used to determine the optimum enzyme concentration. The percent relative activity was used for optimum enzyme concentration.

2.10. Storage

The enzyme homogenate was obtained by filtering the immobilized enzyme and then stored in 0.1 M sodium acetate, pH 5, at 4 °C. Activity was periodically checked for 30 d (1, 6, 12, 18, 24, 30 d).

2.11. Theoretical calculations

Theoretical work involved Gaussian09 RevD.01 and GaussView 6.0, B3LYP, HF, and M06-2x [41–43] with the 6–31++g(d,p) [44,45]. Each

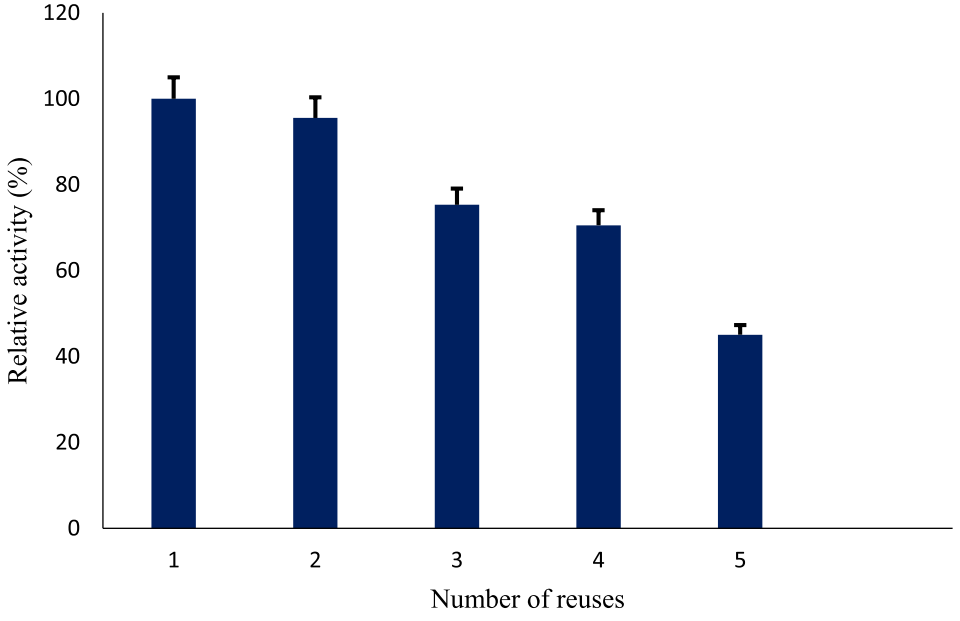

Fig. 6. Reusability of immobilized pectinase.

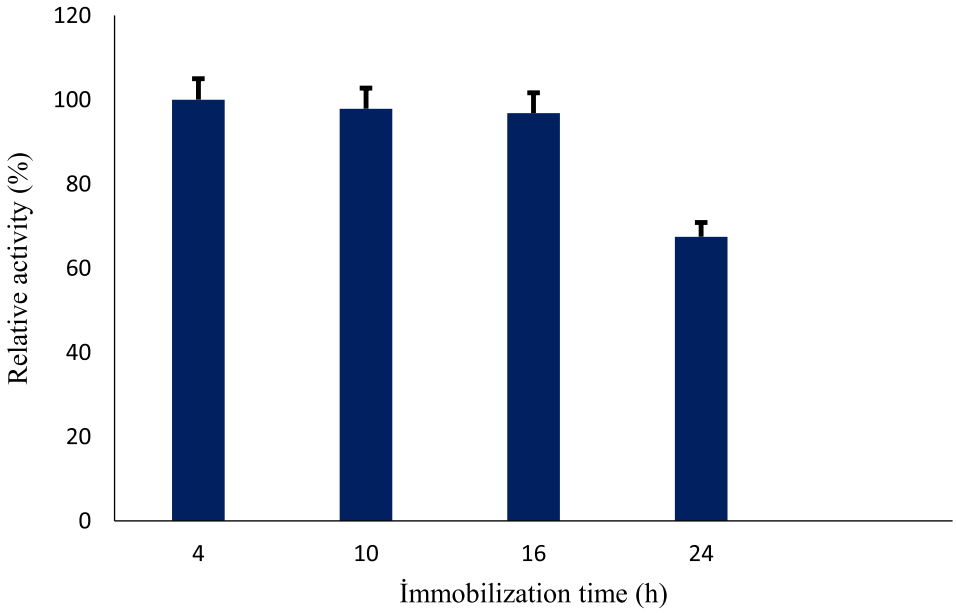

Fig. 7. Effects of immobilization time on free- and immobilized pectinase activity.

of the quantum chemical parameters represented a specific chemical property of the studied molecules (Eqs. 4–6):

$$\chi = -\left(\frac{\partial E}{\partial N}\right)_{v(r)} = \frac{1}{2}(I+A) \cong -\frac{1}{2}(E_{HOMO}+E_{LUMO}) \quad [4]$$

$$\eta = -\left(\frac{\partial^2 E}{\partial N^2}\right)_{v(r)} = \frac{1}{2}(I-A) \cong -\frac{1}{2}(E_{HOMO}-E_{LUMO}) \quad [5]$$

$$\sigma = 1/\eta\omega = \chi^2/2\eta\varepsilon = 1/\omega \quad [6]$$

Molecular docking calculations were reiteratively performed in a Schrödinger's Maestro Molecular modelling software (version 12.8) [46]. This work enabled us to identify the active sites of the molecules. Initially, the protein and molecules were prepared using modules [47] and LigPrep [48], respectively. Prepared proteins and molecules were interacted using the Glide ligand docking tool [49]. Finally, the Qik-prop module [50] was used to execute ADME/T.

3. Results and discussion

3.1. Morphological analyses

3.1.1. SEM analysis

Surface morphologies of the CAC composite, before and after immobilization, were visualized (Fig. 1). Distinct features were visualized on enzyme-immobilized beads. Patent surface coarseness seen before immobilization (Fig. 1a), appeared to have been enhanced after immobilization and porous structures filled with the pectinase (Fig. 1b).

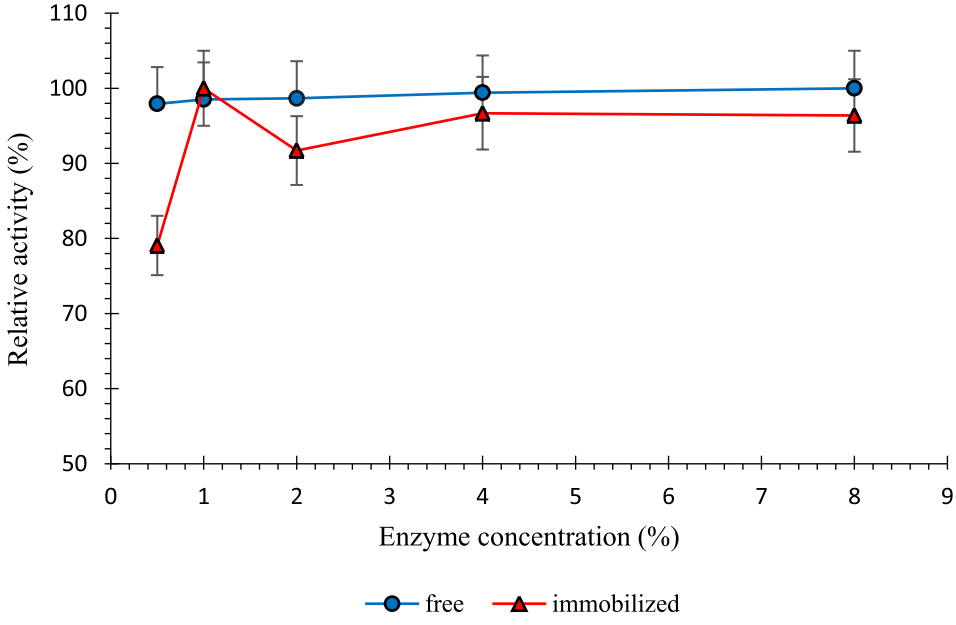

Fig. 8. Effects of enzyme concentration on free- and immobilized pectinase activity.

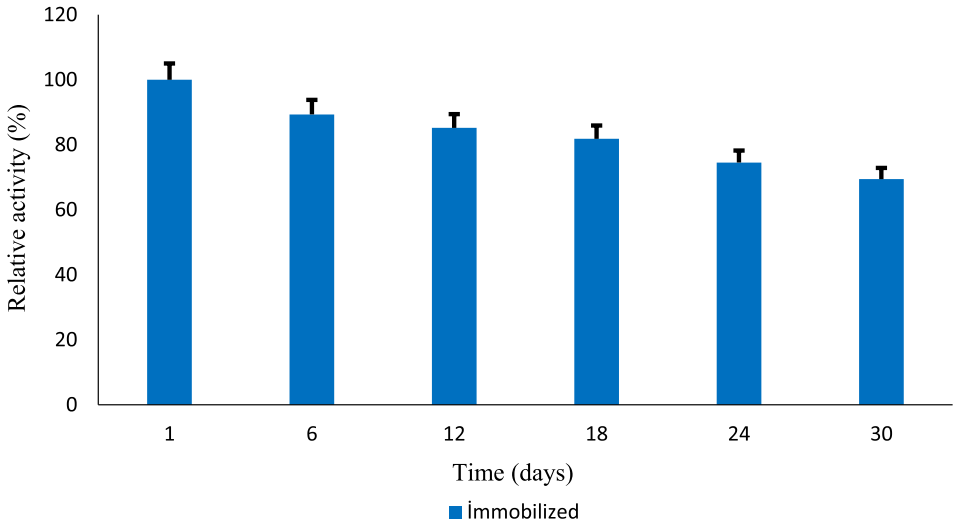

Fig. 9. Effects of storage on immobilized pectinase activity.

3.1.2. FTIR analysis

Two weak peaks at 3692 and 3620 cm^{-1} were O-H stretching vibrations of the hydroxyl groups in the clay, and the wide peak in the 3267 cm^{-1} corresponded to hydroxyl groups of the alginate, chitosan, and the enzyme (1a, Fig. 2). The CH stretching vibrations at 2885 cm^{-1} represented the aliphatic regions of the alginate, chitosan, and the enzyme. The C = O stretch at 1614 cm^{-1} indicated amide carbonyl, formed between the amine of chitosan and the carboxylic acid of the enzyme. The signal seen at 1538 cm^{-1} was the N-H bending vibration. The absence of the C = O stretch at 1726 cm^{-1} (8a and 1a) was taken as the proof for the amide formation. The asymmetric stretching vibration of the ester groups (COO) in the composite structure was represented at 1410 cm^{-1}, and a CH_2 bending of the $–CH_2OH$ in the sugar rings, present in the enzyme, alginate, and chitosan structures, was observed at 1379 cm^{-1}. Stretches of the C-O-C bridge in the sugar rings were represented at 1062 cm^{-1} and 1030 cm^{-1}. A Si-O stretching vibrations at 466 cm^{-1} indicated the incorporation of clay in CAC.

3.2. Enzyme assay

The concentration of reducing sugar (galacturonic acid) in the supernatant was read at 575 nm, using D (+)-galacturonic acid monohydrate as the standard [38]. The principle of the method is based on the oxidation of functional aldehyde or ketone groups. Sugars with free aldehyde or ketone groups reduce 3,5-dinitro salicylic acid to 3-amino-5-nitro salicylic acid under alkaline conditions, and produce red-brown colour. The increase in colour intensity is proportional to the amount of reducing sugar [39]. One unit of pectinase activity (IU/mg) is defined as the amount of galacturonic acid (μmol) produced per milligram of pectinase per minute (Table 1). The specific activity of the free enzyme was 0.2274 μmol /mg $protein^{-1}$ min^{-1}, while the specific activity value of the immobilized enzyme is 0.0488 μmol /mg $protein^{-1}$ min^{-1}. All experiments were performed in triplicate and their average were taken.

Immobilization efficiency (44%) was determined by the difference between the amount of initial protein in the incubation medium and the amount of protein in the washes. The amount of enzyme bound to the support material (CAC) was 0,033 mg protein/mg carrier.

3.2.1. Influence of pH

Pectinase activity was meaningfully swayed by pH (Fig. 3), and the hydrolytic reaction was generally sensitive to both the external environment and the charge distribution on the enzyme molecules [50,51]. The pH range between 3.0 and 8.0 (0.1 M potassium phosphate/citric acid pH 3.0–6.0; 0.1 M phosphate pH 7.0–8.0) were utilised for finding the pH–dependent maximum enzyme activity. The optimum pH values for free and immobilized enzymes were 5.0 and 6.0, respectively. The decrease in the relative activity of the free enzyme was 1.33%, while it was 20.34% in the immobilized enzyme. After covalent binding of pectinase to chitosan beads, some conformational changes in its three-dimensional structure might have occurred, and these changes might also be the main reason for the decrease in the relative activity [40,52].

3.2.2. The role of the temperature

The optimum temperature for the free-and bound pectinases were 50 °C and 60 °C, respectively (Fig. 4). Thus, immobilization appeared to increase the thermal stability of the immobilized pectinase [53]. Beside immobilization, thermal stability might have also been rendered by the physical confinement of pectinase into the composite particles [54].

3.2.3. Kinetic factors

The kinetic parameter values for free- and immobilized enzyme were presented (Table 2, Fig. 5).

Low K_m values indicated high substrate affinity of the enzyme. Thus, the higher K_m of the immobilized pectinase implied that the immobilized enzyme had a relatively lower affinity for its substrate. This finding could be attributed to a slightly negative effect of the immobilization on the pectinolytic activity [55,56]. For similar reasons, the V_{max} of the immobilized pectinase was also lower than that of the free enzyme [57,52].

Increasing K_m and decreasing V_{max} values after immobilization have been reported in the literature, in which K_m and V_{max} for the free enzyme were 6.73 mg/ml and 0.311 mg/ml.min, for the immobilized enzyme, K_m and Vmax were 7.71 mg/ml and 0.303 mg/ml.min, respectively [52].

3.2.4. Reusability

İmmobilized pectinase retained more than 45% of its initial activity after 5 repetitive reuse (Fig. 6). This decrease in immobilized pectinase activity may have resulted from the enzyme detachment or some mechanical damage introduced into the enzyme's active conformation [40,58]. Activity loss, after immobilization, also reported in the literature could be exemplified. In covalent immobilization of pectinase on sodium alginate support, the immobilized enzyme has been reusable and it retained 80% of its initial activity after 11 series of reactions [59]. In a study of immobilization of free pectinase on polystyrene resin beads by cross-linking with glutaraldehyde, the enzyme kept 54.6% of its initial activity after six reuse cycles [60]. *B. subtilis* pectinase, immobilized on an iron oxide nanocarrier, has preserved 90% of its initial activity after

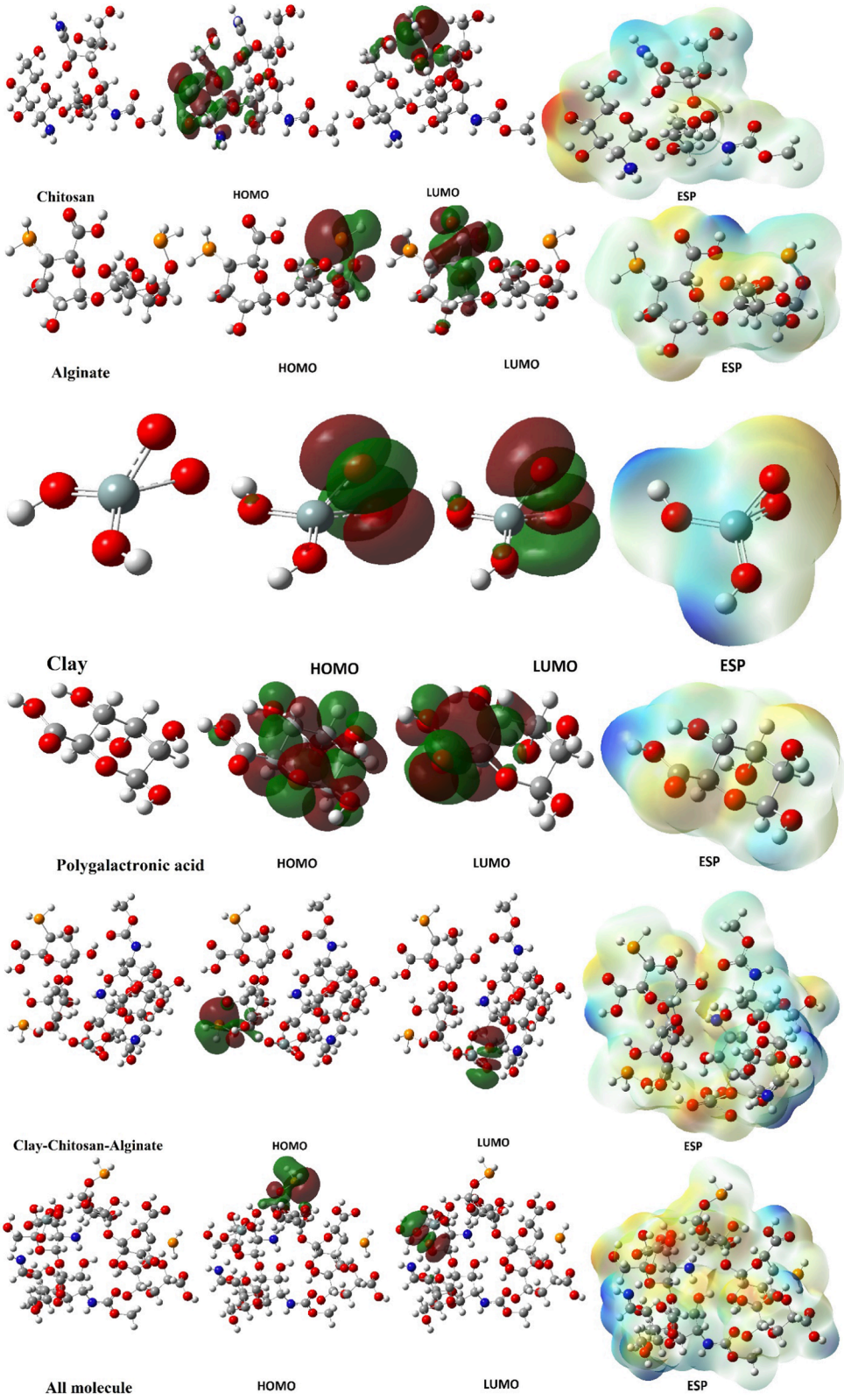

Fig. 10. Representations of optimized structure HOMO, LUMO and ESP of molecules.

Table 3
The calculated quantum chemical parameters of molecules.

	E_{HOMO}	E_{LUMO}	I	A	ΔE	η	μ	χ	Pİ	ω	ε	dipol	Energy
HF/6–31 g LEVEL													
2a	−9.503	1.807	9.503	−1.807	11.310	5.655	0.177	3.848	−3.848	1.309	0.764	12.535	−127154.967
5a	−10.001	3.823	10.001	−3.823	13.824	6.912	0.145	3.089	−3.089	0.690	1.449	1.410	−55361.381
6a	−6.653	1.260	6.653	−1.260	7.913 + i	3.957	0.253	2.696	−2.696	0.919	1.088	15.861	−55833.440
7a	−12.133	3.926	12.133	−3.926	16.059	8.030	0.125	4.104	−4.104	1.049	0.954	5.518	−15956.176
8a	−11.097	4.520	11.097	−4.520	15.616	7.808	0.128	3.289	−3.289	0.693	1.444	2.881	−20482.399
9a	−9.492	1.809	9.492	−1.809	11.301	5.651	0.177	3.842	−3.842	1.306	0.766	12.751	−147637.439

2a: Composite, 5a: Alginate, 6a: chitosan, 7a: clay, 8a: polygalactronic acid, 9a: all molecules.

Table 4
Thermodynamic parameters value of molecules.

1	E	H	G
2a	−127150.2429	−127150.2172	−127154.9672
5a	−55359.20728	−55359.18157	−55361.38171
6a	−55830.55693	−55830.53124	−55833.44079
7a	−15955.23085	−15955.20516	−15956.17648
8a	−20481.07042	−20481.04473	−20482.39916
9a	−147632.0151	−147631.9894	−147637.4397

Table 5
Thermodynamic parameters value of two complexes.

	ΔE	ΔH	ΔG
2a	−5.2478	−5.2992	−3.9682
9a	−5.9496	−6.0267	−4.0415

15 times reuse [61].

3.2.5. Immobilization time and enzyme concentration

Enzyme immobilization reactions were performed at differing time periods (4,10,16, and 24 h). The best time course was 4 h (Fig. 7).

In enzyme activity experiments, different amounts of enzymes were used to determine the best enzyme concentration. Increasing free enzyme concentration also increased the relative activity. Optimum enzyme concentration was found to be 10 mg/ml in the immobilized enzyme (Fig. 8).

3.2.6. Storage

Immobilized- and free enzymes were stored in 0.1 M sodium acetate, pH 5, for 30 d at 4 °C, and their relative activities were determined (Fig. 9). It was attested that the immobilized enzyme retained approximately 67% of its initial activity at the 30th d.

3.3. Theoretical calculations

ESP representations of the molecules visualised their electron-rich (red) and electron-poor (blue) regions (Fig. 10) [62].

Each of the molecules had a specific energy and numerical values of many parameters (Table 3). New and more effective groups of molecules were tried to form by the combination of these molecules, and their thermodynamic parameters did not provide any indications as to the spontaneity of formation (Table 4).

Numerical values of each of the molecules were also presented (Table 5). ΔE, ΔH, and ΔG were calculated using the following equations (Eqs. 7–9):

$$\Delta E = \sum E_{complex} - \sum E_{molecule} \quad [7]$$

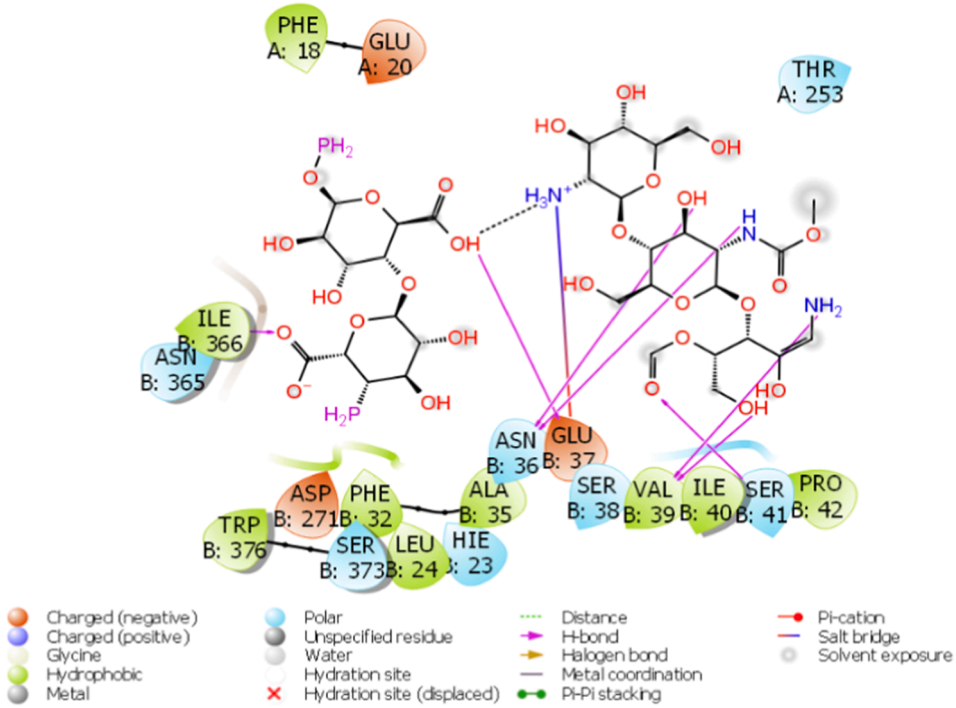

Fig. 11. Presentation interactions of composite molecules with 3K4P.

Fig. 12. Presentation interactions of composite molecules with 3K4P.

Table 6
Numerical values of the docking parameters of molecule against enzymes.

3K4P	Docking Score	Glide ligand efficiency	Glide hbond	Glide evdw	Glide ecoul	Glide emodel	Glide energy	Glide einternal	Glide posenum
2a	−8.05	−0.12	−0.90	−37.46	−29.22	−98.02	−66.68	24.78	76
5a	−3.30	−0.13	−0.29	−16.23	−10.18	−23.16	−26.42	10.38	15
6a	−5.45	−0.14	−0.64	−19.00	−29.76	−64.38	−48.76	16.15	264
7a	−2.97	−0.59	−0.14	2.89	−4.79	−5.18	−1.90	0.01	163
8a	−3.76	−0.29	0.00	−6.86	−7.95	−13.23	−14.82	3.80	2
9a	−5.85	−0.07	−1.10	−49.32	−23.18	−87.86	−72.50	21.30	221
7BLY	Docking Score	Glide ligand efficiency	Glide hbond	Glide evdw	Glide ecoul	Glide emodel	Glide energy	Glide einternal	Glide posenum
2a	−5.25	−0.08	−0.37	−38.87	−15.66	−66.99	−54.53	11.50	26
5a	7.38	0.28	−0.29	−20.76	−16.82	−45.01	−37.58	5.61	10
6a	−5.26	−0.14	−0.55	−14.44	−26.67	−46.93	−41.11	19.71	62
7a	–	–	–	–	–	–	–	–	–
8a	–	–	–	–	–	–	–	–	–
9a	–	–	–	–	–	–	–	–	–
1JIJ	Docking Score	Glide ligand efficiency	Glide hbond	Glide evdw	Glide ecoul	Glide emodel	Glide energy	Glide einternal	Glide posenum
2a	−3.10	−0.11	0.00	−27.87	−3.80	−35.76	−31.67	3.67	52
5a	−6.34	−0.23	0.00	−49.89	−3.28	−69.73	−53.17	3.68	375
6a	−6.00	−0.21	0.00	−38.05	−2.89	−54.37	−40.94	1.26	−6.00
7a	–	–	–	–	–	–	–	–	–
8a	–	–	–	–	–	–	–	–	–
9a	–	–	–	–	–	–	–	–	–

$$\Delta H = \sum E_{complex} - \sum E_{molecule} \quad [8]$$

$$\Delta G = \sum E_{complex} - \sum E_{molecule} \quad [9]$$

Energy E, the sum of electronic and thermal energies, is an important thermodynamic parameter that represents the sum of E_0, E_{vib}, E_{rot}, and E_{transl} energies. Energy H, on the other hand, is the sum of all kinds of energies stored within the structure. The energy G is calculated by substrating these two former total energy values [63].

The composite molecule (CAC) consisted of three molecules, chitosan, alginate, and clay. The Gibbs free energy value of the 2a molecule was negative, −3.9682, (Table 5), indicating that these three molecules assembled spontaneously. Similarly, the free energy of the 9a molecule, formed by adding a polygalactronic acid moiety, was also negative, −4.0415.

Although individual molecules showed antimicrobial activity, they could not show any activity when they came together.

Molecular docking calculations examine the interactions of molecules with proteins. With the increase of these interactions the activity of the molecules also increases and this can inhibit the proteins. It was observed that hydrogen bonds, polar and hydrophobic interactions, π-π and halogen bond interactions occurred between molecules and proteins (Figs. 11 and 12) [64]. Many parameters were calculated, and each of them provided supportive insight (Table 6). The first parameter that determined the activities of the molecules was the docking score. Glide hbond, Glide evdw, and Glide ecoul parameters yielded numerical values of interactions between molecules and proteins [65]. Glide emodel, Glide energy, Glide einternal, and Glide posenum provided information on the interaction between molecules and proteins [66].

ADME/T analysis (absorption, distribution, metabolism, excretion, and toxicity) was performed to examine the effects and responses of these studied molecules in human metabolism. The parameters

Table 7
ADME properties of molecule.

	2a	5a	6a	7a	8a	9a	Referance Range
mol_MW	–	418	558	94	194	–	130–725
dipole (D)	–	2.7	7.5	3.3	5.9	–	1.0–12.5
SASA	–	530	760	232	359	–	300–1000
FOSA	–	128	314	21	84	–	0–750
FISA	–	266	446	210	275	–	7–330
PISA	–	0	0	0	0	–	0–450
WPSA	–	136	0	0	0	–	0–175
volume (A^3)	–	993	1488	311	571	–	500–2000
donorHB	–	9	11	2	4	–	0–6
accptHB	–	16.6	25.7	5.7	9.5	–	2.0–20.0
glob (Sphere = 1)	–	0.9	0.8	1.0	0.9	–	0.75–0.95
QPpolrz (A^3)	–	26.5	39.9	5.0	13.5	–	13.0–70.0
QPlogPC16	–	12.6	17.6	3.0	6.6	–	4.0–18.0
QPlogPoct	–	31.6	44.3	7.7	16.2	–	8.0–35.0
QPlogPw	–	30.0	41.4	9.8	16.6	–	4.0–45.0
QPlogPo/w	–	−1.1	−5.4	−2.0	−1.8	–	−2.0–6.5
QPlogS	–	−2.1	0.7	0.0	−0.9	–	−6.5–0.5
CIQPlogS	–	−1.4	0.5	−0.1	−0.4	–	−6.5–0.5
QPlogHERG	–	0.6	−5.0	−2.2	−0.9	–	*
QPPCaco (nm/sec)	–	2	0	100	6	–	**
QPlogBB	–	−1.9	−4.6	−1.1	−1.9	–	−3.0–1.2
QPPMDCK (nm/sec)	–	5	0	41	3	–	**
QPlogKp	–	−5.4	−9.8	−5.2	−6.1	–	Kp in cm/hr
IP (ev)	–	8.9	9.7	10.7	10.9	–	7.9–10.5
EA (eV)	–	−0.3	−0.8	4.4	−0.4	–	−0.9–1.7
#metab	–	6	8	0	4	–	1–8
QPlogKhsa	–	−1.3	−2.0	−1.0	−1.1	–	−1.5–1.5
Human Oral Absorption	–	1	1	2	2	–	–
Percent H. Oral Absorp.	–	0	0	51.3	30.3	–	***
PSA	–	191	306	82	143	–	7–200
RuleOfFive	–	2	3	0	0	–	Maximum is 4
RuleOfThree	–	1	2	0	1	–	Maximum is 3
Jm	–	0.0	0.0	0.6	0.0	–	–

* corcern below −5, **<25 is poor and >500 is great, *** <25% is poor and >80% is high.

calculated here were divided into two groups, indicating chemical and biological properties of molecules.

The ADME/T values of two important complex groups that could not be calculated were shown (Table 7), because the number of complex atoms was high and because the molecules in the complex could not be covalently bonded to each other. Although the calculated chemical and biological parameters of the six different molecules, the numerical values of the RuleOfFive [67,68] and RuleOfThree [69], were found within the desired category as to their compatibility with human metabolism, only two of these parameters indicated their usability as drugs.

4. Conclusions

A chitosan-alginate-clay composite was prepared using double crosslinkers, epichlorohydrin and sodium tripolyphosphate. *Aspergillus niger* pectinase was crosslinked on this matrix. Optimum pH points were determined. In both bound- and unbound state, the shift above the optimum pH, 5 and 6, respectively, decreased the pectinolytic activity. This decrease was more enhanced in the unbound state. Immobilization increased the optimum temperature from 50 to 60 °C. Kinetic and theoretical studies were in agreement, indicating that three-parted CAC composite was spontaneously formed as the Gibbs free energy values were negative. Reiterative use could be possible as the immobilized enzyme preserved 45% of its initial activity after five reuses. As to its shelf life, the enzyme kept 67% of its activity after 30 d storage in solution at 4 °C. The ADME/T values indicated that CAC was compatible with the human metabolism and could be used as a drug carrier.

Funding

The study was funded by the Sivas Cumhuriyet University Scientific Research Projects, Turkey (No. F-2022-660).

Declaration of Competing Interest

The authors declare that they have no known competing financial interests or personal relationships that could have appeared to influence the work reported in this paper.

Data availability

No data was used for the research described in the article.

References

[1] P. Anastas, J.C. Warner, Green, Chemistry Theory and Practice, Oxford University press, Great Britain. (2000).
[2] R.A. Sheldon, J.M. Woodley, Role of biocatalysis in sustainable chemistry, Chem. Rev. 118 (2) (2018) 801–838.
[3] A. Illanes, A. Cauerhff, L. Wilson, G.R. Castro, Recent trends in biocatalysis engineering, Bioresour. Technol. 115 (2012) 48–57.
[4] S. Jemli, D. Ayadi-Zouari, H.B. Hlima, S. Bejar, Biocatalysts: application and engineering for industrial purposes, Crit. Rev. Biotechnol. 36 (2) (2016) 246–258.
[5] F.T.T. Cavalcante, F.S. Neto, I. Rafael de Aguiar Falcão, J. Erick da Silva Souza, L. S. de Moura Junior, P. da Silva Sousa, T.G. Rocha, I.G. de Sousa, P.H. de Lima Gomes, M.C.M. de Souza, J.C.S. dos Santos, Opportunities for improving biodiesel production via lipase catalysis, Fuel 288 (2021) 119577.
[6] E. Busto, V. Gotor-Fernández, V. Gotor, Hydrolases: catalytically promiscuous enzymes for non-conventional reactions in organic synthesis, Chem. Soc. Rev. 39 (2010) 4504–4523.
[7] R. Sharma, Y. Chisti, U.C. Banerjee, Production, purification, characterization, and applications of lipases, Biotechnol. Adv. 19 (8) (2001) 627–662.
[8] W.K. Chui, L.S.C. Wan, Prolonged retention of cross-linked trypsin in calcium alginate microspheres, J. Microencapsul. 14 (1) (1997) 51–61.
[9] F. Rafiee, M. Rezaee, Different strategies for the lipase immobilization on the chitosan based supports and their applications, Int. J. Biol. Macromol. 179 (2021) 170–195.
[10] P. Adlercreutz, Immobilisation and application of lipases in organic media, Chem. Soc. Rev. 42 (2013) 6406–6436.
[11] C. Mateo, J.M. Palomo, G. Fernandez-Lorente, J.M. Guisan, R. Fernandez-Lafuente, Improvement of enzyme activity, stability and selectivity via immobilization techniques, Enzym. Microb. Technol. 40 (6) (2007) 1451–1463.
[12] U. Hanefeld, L. Gardossi, E. Magner, Understanding enzyme immobilisation, Chem. Soc. Rev. 38 (2) (2009) 453–468.
[13] J. Boudrant, J.M. Woodley, R. Fernandez-Lafuente, Parameters necessary to define an immobilized enzyme preparation, Process Biochem. 90 (2020) 66–80.
[14] J. Zdarta, A.S. Meyer, T. Jesionowski, M. Pinelo, A general overview of support materials for enzyme immobilization: characteristics, properties, practical utility, Catalysts 8 (2018) 92.
[15] B. Krajewska, Application of chitin-and chitosan-based materials for enzyme immobilizations: a review, Enzym. Microb. Technol. 35 (2-3) (2004) 126–139.
[16] E. Górecka, M. Jastrzębska, Immobilization techniques and biopolymer carriers, Biotechnol. Food Sci. 75 (2011) 65–86.
[17] S. Datta, L.R. Christena, Y.R.S. Rajaram, Enzyme immobilization: an overview on techniques and support materials, 3, Biotech 3 (2013) 1–9.
[18] N.R. Mohamad, N.H.C. Marzuki, N.A. Buang, F. Huyop, R.A. Wahab, An overview of technologies for immobilization of enzymes and surface analysis techniques for immobilized enzymes, Biotechnol. Biotechnol. Equip. 29 (2) (2015) 205–220.
[19] R. Sheldon, Cross-linked enzyme aggregates (CLEAs): stable and recyclable biocatalysts, Biochem.. Soc. Trans. 35 (2007) 1583–1587.
[20] P. Tufvesson, J. Lima-Ramos, M. Nordblad, J.M. Woodley, Guidelines and cost analysis for catalyst production in biocatalytic processes, Org. Process Res. Dev. 15 (1) (2011) 266–274.
[21] H. Horchani, I. Aissa, S. Ouertani, Z. Zarai, Y. Gargouri, A. Sayari, Staphylococcal lipases: biotechnological applications, J. Mol. Catal. B Enzym. 76 (2012) 125–132.
[22] W. Tischer, F. Wedekind, Immobilized enzymes: methods and applications, Biocatalysis-from discovery to application. (1999) 95–126.
[23] K. Kurita, Controlled functionalization of the polysaccharide chitin, Prog. Polym. Sci. 26 (9) (2001) 1921–1971.
[24] M.G. Peter, Applications and environmental aspects of chitin and chitosan, J. Macromol. Sci., Pure Appl. Chem. 32 (1995) 629–640.
[25] D.M. Liu, J. Chen, Y.P. Shi, Advances on methods and easy separated support materials for enzymes immobilization, Trends Anal. Chem. 102 (2018) 332–342.
[26] A. Tas, B. Tüzün, A.N. Khalilov, P. Taslimi, T. Ağbektas, N.K. Cakmak, In vitro cytotoxic effects, in silico studies, some metabolic enzymes inhibition, and

vibrational spectral analysis of novel β-amino alcohol compounds, J. Mol. Struct. 1273 (2023), 134282.
[27] M. Chalkha, A.A. el Hassani, A. Nakkabi, B. Tüzün, M. Bakhouch, A.T. Benjelloun, M. El Yazidi, Crystal structure, Hirshfeld surface and DFT computations, along with molecular docking investigations of a new pyrazole as a tyrosine kinase inhibitor, J. Mol. Struct. 1273 (2023), 134255.
[28] A.J. Oakley, The structure of Aspergillus niger phytase PhyA in complex with a phytate mimetic, Biochem. Biophys. Res. Commun. 3974 (2010) 745–749.
[29] M. Bonin, L. Hameleers, L. Hembach, T. Roret, S. Cord-Landwehr, G. Michel, B. M. Moerschbacher, In silico and in vitro analysis of an Aspergillus niger chitin deacetylase to decipher its subsite sugar preferences, J. Biol. Chem. 2974 (2021).
[30] X. Qiu, C.A. Janson, W.W. Smith, S.M. Green, P. McDevitt, K. Johanson, P. Carter, M. Hibbs, C. Lewis, A. Chalker, A. Fosberry, J. Lalonde, J. Berge, P. Brown, C.S. V. Houge-Frydrych, R.L. Jarvest, Crystal structure of Staphylococcus aureus tyrosyl-tRNA synthetase in complex with a class of potent and specific inhibitors, Protein Sci. 10 (10) (2001) 2008–2016.
[31] F. Amin, A. Mohsin, H.N. Bhatti, M. Bilal, Production, thermodynamic characterization, and fruit juice quality improvement characteristics of an Exopolygalacturonase from Penicillium janczewskii, Biochim. Biophys. Acta Protein Proteomics. 1868 (2020), 140379.
[32] X. Zeng, E. Ruckenstein, Cross-linked macroporous chitosan anion-exchange membranes for protein separations, J. Membr. Sci. 1482 (1998) 195–205.
[33] A. Dinçer, A. Telefoncu, Improving the stability of cellulase by immobilization on modified polyvinyl alcohol coated chitosan beads, J. Mol. Catal. B Enzym. 45 (1–2) (2007) 10–14.
[34] W.S. Wan Ngah, L.C. Teong, C.S. Wong, M.A.K.M. Hanafiah, Preparation and characterization of chitosan–zeolite composites, J. Appl. Polym. Sci. (2012) 2417–2425.
[35] H.F. Çetinkaya, M.S. Cebeci, S. Kaya, N.S. Jalbani, M.M. Maslov, R. Marzouki, Removal of erythrosine B dye from wastewater using chitosan boric acid composite material: Experimental and density functional theory findings, J. Phys. Org. Chem. (2022) e4400.
[36] S. Romo-Sánchez, M. Arévalo-Villena, E. García Romero, H.L. Ramirez, A. Briones Pérez, Immobilization of β-glucosidase and its application for enhancement of aroma precursors in Muscat wine, Food Bioproc. Tech.. 7 (5) (2014) 1381–1392.
[37] M.M. Bradford, A rapid and sensitive method for the quantitation of microgram quantities of protein utilizing the principle of protein-dye binding, Anal. Biochem. 72 (1–2) (1976) 248–254.
[38] G.L. Miller, Use of dinitrosalicylic acid reagent for determination of reducing sugar, Anal. Chem. 31 (3) (1959) 426–428.
[39] P. Bernfeld, Amylases α and β, Methods. Enzymol. 1 (1959) 149–158.
[40] M. Mohammadi, M.K. Heshmati, K. Sarabandi, M. Fathi, L.T. Lim, H. Hamishehkar, Activated alginate-montmorillonite beads as an efficient carrier for pectinase immobilization, Int. J. Biol. Macromol. 137 (2019) 253–260.
[41] A.D. Becke, Density-functional thermochemistry. I The effect of the exchange-only gradient correction, J. Chem. Phys. 96 (3) (1992) 2155–2160.
[42] D. Vautherin, D.M. Brink, Hartree-Fock calculations with Skyrme's interaction. I. Spherical nuclei, Phys. Rev. C. 5 (3) (1972) 626–647.
[43] E.G. Hohenstein, S.T. Chill, C.D. Sherrill, Assessment of the performance of the M05–2X and M06–2X exchange-correlation functionals for noncovalent interactions in biomolecules, J. Chem. Theory Comput. 4 (12) (2008) 1996–2000.
[44] M. Rezaeivala, M. Bozorg, N. Rafiee, K. Sayin, B. Tuzun, Corrosion inhibition of Carbon Steel using a new morpholine-based ligand during acid pickling: Experimental and theoretical studies, Inorg. Chem. Commun. 148 (2023) 110323.
[45] G. Sarkı, B. Tüzün, D. Ünlüer, H. Kantekin, Synthesis, characterization, chemical and biological activities of 4-(4-methoxyphenethyl)-5-benzyl-2-hydroxy-2H-1, 2, 4-triazole-3 (4H)-one phthalocyanine derivatives, Inorg. Chim. Acta 545 (2023), 121113.
[46] Schrödinger Release (2021-3): Maestro, Schrödinger, LLC, New York, NY, (2021).
[47] Schrödinger Release (2019-4): Protein Preparation Wizard; Epik, Schrödinger, LLC, New York, NY, (2016); Impact, Schrödinger, LLC, New York, NY, (2016); Prime, Schrödinger, LLC, New York, NY, (2019).
[48] Schrödinger Release (2021-3): LigPrep, Schrödinger, LLC, New York, NY, (2021).
[49] M.K. Erdogan, R. Gundogdu, Y. Yapar, I.H. Gecibesler, M. Kirici, L. Behcet, P. Taslimi, In vitro anticancer, antioxidant and enzyme inhibitory potentials of endemic Cephalaria elazigensis var. purpurea with in silico studies. Journal of Biomolecular Structure and Dynamics. (2023) 1-13.
[50] Schrödinger Release (2021-3): QikProp, Schrödinger, LLC, New York, NY, (2021).
[51] U.V. Sojitra, S.S. Nadar, V.K. Rathod, for fruit juice clarification, Food Chem. 213 (2016) 296–305.
[52] X.Y. Dai, L.M. Kong, X.L. Wang, Q. Zhu, K. Chen, T. Zhou, Preparation, characterization and catalytic behavior of pectinase covalently immobilized onto sodium alginate/ graphene oxide composite beads, Food Chem. 253 (2018) 185–193.
[53] S.D. Gür, N. İdil, N. Aksöz, Optimization of enzyme co-immobilization with sodium alginate and glutaraldehyde-activated chitosan beads, Appl. Biochem. Biotechnol. 184 (2018) 538–552.
[54] F. Kara, G. Demirel, H. Tümtürk, Immobilization of urease by using chitosan–alginate and poly (acrylamide-co-acrylic acid)/κ-carrageenan supports, Bioprocess Biosyst. Eng. 29 (2006) 207–211.
[55] T. Bahar, A. Tuncel, Immobilization of α-chymotrypsin onto newly produced poly (hydroxypropyl methacrylate-co-methacrylic acid) hydrogel beads, React. Funct. Polym. 44 (2000) 71–78.
[56] A. Homaei, Immobilization of Penaeus merguiensis alkaline phosphatase on gold nanorods for heavy metal detection, Ecotoxicol. Environ. Saf. 136 (2017) 1–7.
[57] S.S. Nadar, V.K. Rathod, Magnetic macromolecular cross linked enzyme aggregates (CLEAs) of glucoamylase, Enzyme Microb. Technol. 83 (2016) 78–87.
[58] M. Bilal, T. Rasheed, H.M.N. Iqbal, H. Hu, W. Wang, X. Zhang, Novel characteristics of horseradish peroxidase immobilized onto the polyvinyl alcohol-alginate beads and its methyl orange degradation potential, Int. J. Biol. Macromol. 105 (2017) 328–335.
[59] T. Li, N.a. Wang, S. Li, Q. Zhao, M. Guo, C. Zhang, Optimization of covalent immobilization of pectinase on sodium alginate support, Biotechnol. Lett 29 (9) (2007) 1413–1416.
[60] Q. Miao, C. Zhang, S. Zhou, L. Meng, L. Huang, Y. Ni, L. Chen, Immobilization and characterization of pectinase onto the cationic polystyrene resin, ACS Omega 6 (47) (2021) 31683–31688.
[61] T. Behram, S. Pervez, M.S. Nawaz, S. Ahmad, A.U. Jan, H.U. Rehman, S. Ahmad, N. M. Khan, F.A. Khan, Development of pectinase based nanocatalyst by immobilization of pectinase on magnetic iron oxide nanoparticles using glutaraldehyde as crosslinking agent, Molecules 28 (2023) 404.
[62] P. Taslimi, F. Akhundova, M. Kurbanova, F. Türkan, B. Tuzun, A. Sujayev, İ. Gülçin, Biological activity and molecular docking study of some bicyclic structures: antidiabetic and anticholinergic potentials, Polycycl. Aromat. Compd. 42 (9) (2022) 6003–6016.
[63] A.T. Bilgicli, H.G. Bilgicli, A. Günsel, H. Pişkin, B. Tüzün, M.N. Yarasir, M. Zengin, The new ball-type zinc phthalocyanine with SS bridge; Synthesis, computational and photophysicochemical properties, J. Photochem. Photobiol. A Chem. 389 (2020), 112287.
[64] A. Poustforoosh, H. Hashemipour, B. Tüzün, M. Azadpour, S. Faramarz, A. Pardakhty, M.H. Nematollahi, The impact of D614G mutation of SARS-COV-2 on the efficacy of anti-viral drugs: A comparative molecular docking and molecular dynamics study, Curr. Microbiol. 79 (8) (2022) 241.
[65] A. Mermer, M.V. Bulbul, S.M. Kalender, I. Keskin, B. Tuzun, O.E. Eyupoglu, Benzotriazole-oxadiazole hybrid Compounds: Synthesis, anticancer Activity, molecular docking and ADME profiling studies, J. Mol. Liq. 359 (2022), 119264.
[66] H. Kekeçmuhammed, M. Tapera, B. Tüzün, S. Akkoç, Y. Zorlu, E. Sarıpınar, Synthesis, molecular docking and antiproliferative activity studies of a thiazole-based compound linked to hydrazone moiety, Chem. Select. 7 (26) (2022) e202201502.
[67] C.A. Lipinski, Lead-and drug-like compounds: the rule-of-five revolution, Drug Discov. Today Technol. 1 (4) (2004) 337–341.
[68] C.A. Lipinski, F. Lombardo, B.W. Dominy, P.J. Feeney, Experimental and computational approaches to estimate solubility and permeability in drug discovery and development settings, Adv. Drug Deliv. Rev. 23 (1997) 3–25.
[69] W.J. Jorgensen, E.M. Duffy, Prediction of drug solubility from structure, Adv. Drug Deliv. Rev. 54 (3) (2022) 355–366.